GEOPHYSICAL RESEARCH LETTERS, VOL. 28, NO. 23, PAGES 4467-4470, DECEMBER 1, 2001

Seasonal and Intraseasonal Thermocline Variability in the Central South China Sea

Qinyu Liu, Yinglai Jia, Penghui Liu, Qi Wang

Physical Oceanography Laboratory, Ocean University of Qingdao, Qingdao, China

Peter C. Chu

Department of Oceanography, Naval Postgraduate School, Monterey, CA, U.S.A.

Abstract. Seasonal and intraseasonal variability of thermocline and relative surface height in the central South China Sea (SCS) are investigated using time series data of temperature from three buoys and sea surface height anomaly data from TOPEX/POSEIDON and ERS-1/ERS-2 satellites (T/P-ERS) from Feb. 1998 through Mar. 1999. We found that the thermocline becomes deeper and thinner in winter, owing to a great loss of the heat on the sea surface. This feature is more evident in the northern than the southern part of the central SCS. The intraseasonal variation of the thermocline is mainly controlled by the geostrophic vorticity and is out-of-phase with sea surface height (SSH). Furthermore, we find a double-thermocline phenomenon occurs in the SCS: In spring, owing to maximum net downward heat flux at the surface, with the new thermocline appearing above 80 m and the old thermocline keeping under 80 m deep.

Introduction

The South China Sea (SCS) has a bottom topography that makes it a unique semi-enclosed ocean basin that is temporally forced by a pronounced monsoon wind. The SCS thermohaline structure and associated dynamical mechanisms were investigated by *Chu et al.* [1998, 1999]. The SCS thermocline has an evident seasonal variability [*Xu et al.*, 1993; *Chu et al.*, 1998; *Liu et al.*, 2000]. Using NOAA monthly mean temperature data [Levitus, 1984], *Liu et al.* [2000] found that the thermocline is thinnest and weakest in winter, thickest in spring, and strongest in summer and fall. Such a seasonal variability is affected by Ekman downwelling (upwelling) due to the anticyclonic (cyclonic) wind stress curl [*Chu et al.*, 1998]. The SCS thermocline has an evident intraseasonal variability. For example, a multi-thermocline structure was observed in the southern SCS in September 1994 [*Qiu et al.*, 1996]. Such a multi-thermocline structure has not been found in monthly mean climatogical data and numerical model in the SCS. In this paper, we analyze T/P-ERS satellite SSH anomaly data and temperature data from three ATLAS anchored buoys deployed by the Institute of Oceanography, Taiwan University to search for the mechanism governing the multi-thermocline formation.

Paper number 2001GL013185.
0094-8276/01/2001GL013185$05.00

Data

Temperature

During the South China Sea Monsoon Experiment (SCSMEX), three ATLAS anchored buoys were deployed at SCS1 (18°5.9'N, 115°35.8'E), SCS2 (15°2.6'N, 114°57.3'E) and SCS3 (12°58.5'N, 114°24.5'E) (Fig. 1) to get a long time series (10 min interval) of sea surface meteorological data, ocean temperature, salinity and current data. The data used in this study is from April 20, 1998 to April 8, 1999. The water temperature at 1, 25, 50, 75, 100, 125, 150, 200, 250, 300 and 500 meters was recorded. The data is interpolated using a cubic spline in vertical direction, and the daily mean data have been smoothed using a 7-point running mean.

SSH anomaly

The SSH anomaly data are obtained from Archiving, Validation, and Interpretation of Satellite Data in Oceanography (AVISO), which are merged T/P-ERS altimeter data and are interpolated onto a $0.25^o \times 0.25^o$ grid using the optimum interpolation. The SSH anomaly means the observation of satellite subtracted by climate mean and corrected by getting rid of tide and other errors. It reflects only the variation of the SSH. The mean SSH from 1993 to 1995, which was simulated by the Parallel Ocean Climate Model (POCM) with $1/4^o \times 1/4^o$ resolution ocean general circulation model, has been used to instead of the climate mean observation on the anomaly field from satellite. This mean SSH for the three years is added to the satellite SSH anomaly data and to form the SSH data in this paper.

Seasonal variation of the thermocline in the central SCS

The time-depth section of temperature for the three buoy stations (Fig. 2) shows the spatial and temporal variability of the thermocline. The lighter shade means the vertical temperature gradient is between 0.05 and 0.08°C/m. The darker shade area means the vertical temperature gradient larger than 0.08°C/m. The seasonal thermocline variability at the three buoys has the same characteristics: In winter (especially January - February 1999), the thermocline thickness reaches a minimum value (about 80 m). While in other seasons (April-October 1998), the thermocline is thicker than 100 m. At the end of March 1999, the double thermocline structure occurs in all the three buoy stations. The upper thermocline, appearing at about 40 m, is caused by increase of solar radiation at the sea surface [*Yang et*

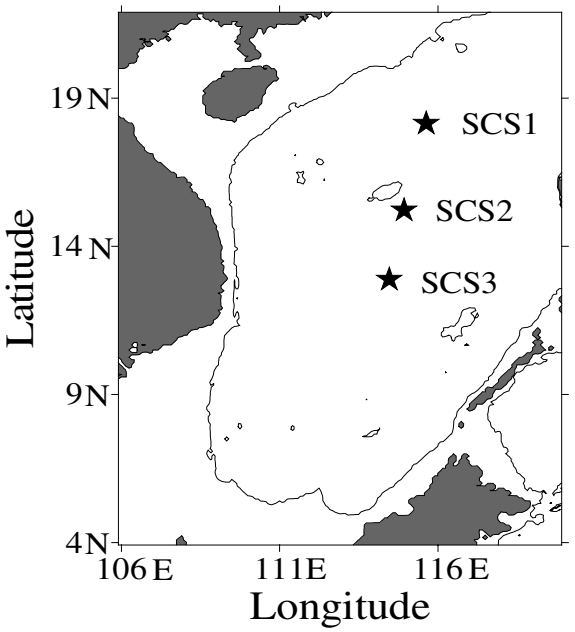

Figure 1. Location of three observational stations in the central SCS (the solid line is 200 m isobath and the five-star means the position).

al., 1999] and reduction of surface evaporation due to atmospheric downdraft caused by anticyclonic wind stress curl in the central SCS [*Liu et al.*, 2001]. Besides, the anticyclonic wind stress curl drives anticyclonic circulation in the upper ocean. This circulation in turn transports surface warm water to the center of the anticyclone, suppresses the upwelling. Weakening of the sea surface wind reduces the vertical mixing. All of these factors are favorable for the rapid increase of SST, and in turn for the formation of a new thermocline in the upper mixed layer during spring. The seasonal variation of the thermocline is most evident in the buoy station SCS1. In addition to the seasonal variability, there is an intraseasonal variation (at about 1-2 months) at all stations.

Thermocline depth, SSH, and stratification

Based on the Fig. 2, we may take the depth of the 22°C isotherm as the thermocline depth. Out-of-phase relationship among the three buoy stations is found from temporal variations of thermocline depth (negative value) to SSH (Fig. 3). The correlation coefficients between the two time series are -0.462 (SCS1), -0.88 (SCS2) and -0.699 (SCS3), respectively. The correlation coefficients are significant with confidence interval exceeding 95%. It has been examined that the two-layer system is dominating baroclinic system in the central SCS. Then we can know some variation information of the thermocline based on variation of the SSH in the central SCS. The ratio of the SSH and thermocline depth anomaly (relative to the mean thermocline depth) can be interpreted as $g'H_2/gH$ in a two layer model [*Gill*, 1982] where g' and g are reduced and normal gravity respectively, H and H_2 are the total depth and the depth of the second layer at rest. Thus, this ratio may indicate the oceanic stratification. The amplitudes of the time series of the 22°C isotherm depth (i.e., maximum thermocline depth anomaly) are 437, 170 and 240 times of that of the SSH at the three stations, which implies different stratifications at the three stations.

Intraseasonal variation of the thermocline and the double-thermocline structure

There are two mechanisms causing the thermocline rising and deepening in intraseasonal scale: surface net heat flux and mesoscale eddies. The mesoscale eddies (space scale is 10-100 km) tend to be in approximate geostrophic balance [*Gill*, 1982], the geostrophic vorticity calculated from SSH may represent the location and strength of the meso-scale eddies. The thermocline changes when an eddy passes by. (When the cyclone eddy passes by, the thermocline rises; and when anticyclone eddy passes by, the thermocline sinks) Thus, thermocline and geostrophic vorticity are related to each other. This is confirmed from a close relationship between the depth of the 22°C isotherm (thermocline depth) and the geostrophic vorticity at all three stations (Fig. 4), with correlation coefficients (more than 95% confidence) of 0.573, 0.512 and 0.481 respectively. Now, we further examine those relationships and investigate the mechanism causing the formation of double thermoclines.

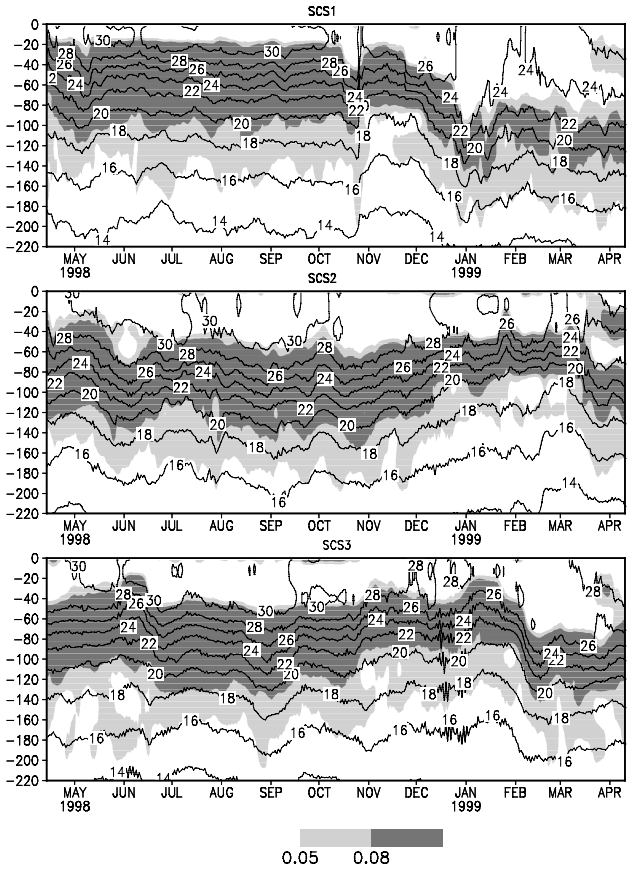

Figure 2. Time-depth sections of temperature from the three buoys from April 1998 to March 1999: (a) SCS1; (b) SCS2; (c) SCS3. The shaded area denotes the thermocline. The lighter shade means the vertical temperature gradient is between 0.05°C/m and 0.08°C/m. The darker shade means the vertical temperature gradient is larger than 0.08°C/m.

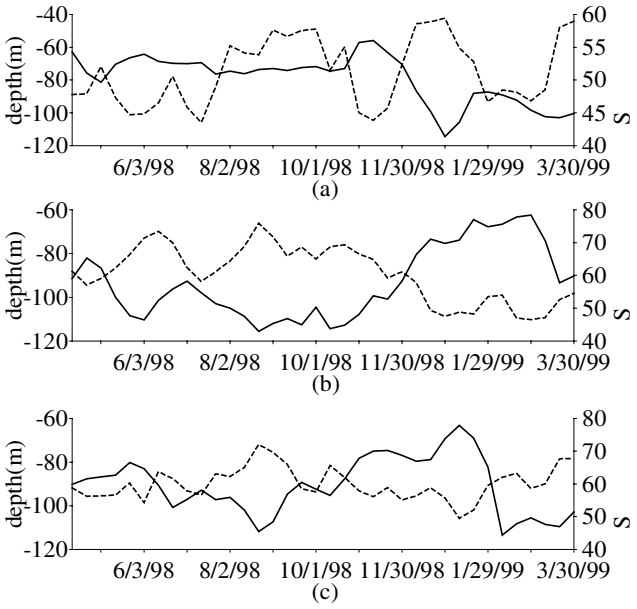

Figure 3. Time series of 22°C isotherm depth (solid line) and sea surface height (dashed line) at (a) SCS1; (b)SCS2; (c)SCS3.

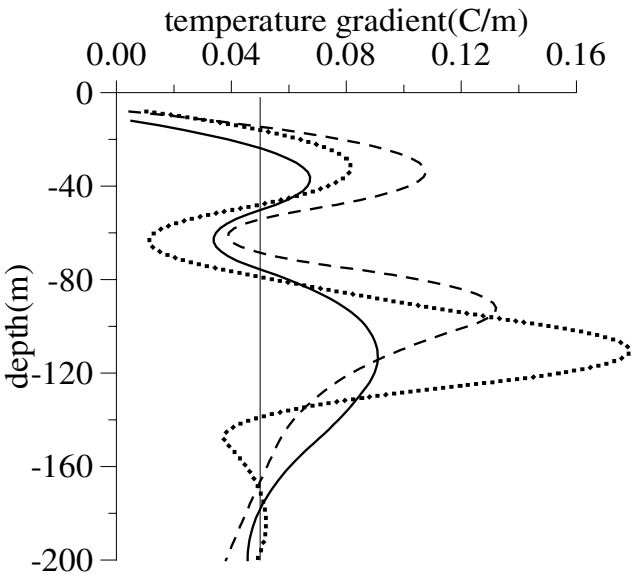

Figure 5. Vertical temperature gradient at SCS1 on April 1 (solid line); at SCS2 on April 1 (dashed line); (c) at SCS3 on March 27 (dotted line).

SCS1

At the station SCS1, from end of April to early May 1998, the geostrophic vorticity is negative (Fig. 4a) which facilitates the deepening of the thermocline (Fig. 2a). The upper boundary of the thermocline is deeper than 20 m in May. After 10 October 1998, the entire thermocline sinks, its lower boundary is below 190 m on 19 October 1998, around 20m depression (Fig. 2a) at the station SCS1. We can not sure what could make the thermocline to sink, but it has some relation with the decrease positive geostrophic vorticity at the station SCS1 (Fig. 4a). After October 20, 1998, the entire thermocline rises rapidly. In early November 1998, the upper and lower boundaries of the thermocline are located at 20 m, and 90 m, respectively. The lower boundary rises 100 m from the end of October (Fig. 2a). In December 1998, the entire thermocline deepens due to strong surface heat loss and the negative geostrophic vorticity. From the end of December 1998 to early January 1999, because of the effect of heat loss [*Yang et al.*, 1999] and negative vorticity of SSH (Fig. 4), the upper boundary of the thermocline reached the deepest of the year (80 m), which is even deeper than the lower boundary in early November. From January to March 1999, negative geostrophic vorticities push down the existing thermocline (old). In March, the maximum monthly mean downward surface net heat flux (strong solar radiation) rapidly increases SST [*Yang et al.*, 1999], shallows the mixed layer and causes the formation of a new upper thermocline at 40 m (Fig. 5), and leads to the occurrence of the double thermoclines at the end of March 1999 (Fig.2a and Fig. 5). The lower thermocline is the "old" thermocline (the lower boundary remains at 180 m) formed in winter and preserved by the anticyclinc eddy corresponding with negative geostrophic vorticity (Fig. 4a). The thermocline gap is above 30 m (from -50 m to -80 m) (Fig. 5)

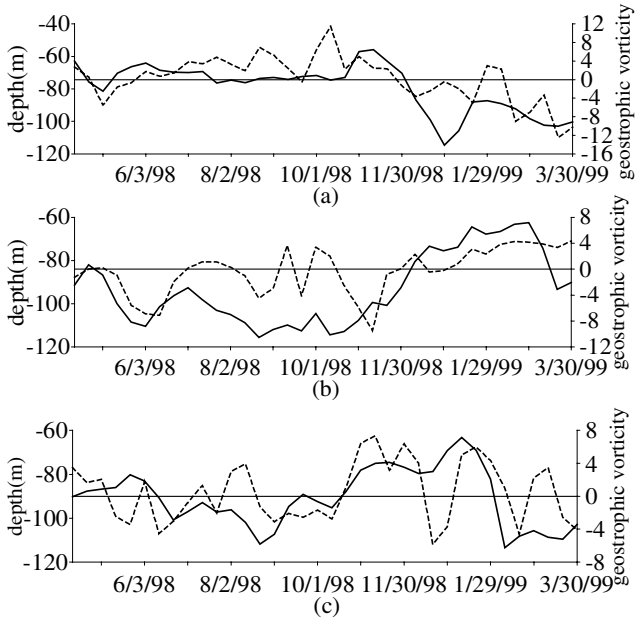

Figure 4. Time series of 22°C isotherm depth (solid line) and geostrophic vorticity (dashed line) at (a) SCS1; (b)SCS2; (c)SCS3.

SCS2

There is intraseasonal variation too in this period for station SCS2. In early June 1998, the geostrophic vorticity become negative ($-7\times10^{-8}s^{-1}$)(Fig. 4b). As a result, the upper boundary of the thermocline deepens from 20 m (early May 1998) to 70 m (early June 1998), while the lower boundary of the thermocline deepens from 140 m (early May 1998) to 180 m (early June 1998). With the weakening of the negative geostrophic vorticity in early July 1998, the upper boundary of thermocline rises from 60 m to 40 m from June 1 to early July 1998 (Fig. 2b). From mid October to early December 1998, an anticyclonic eddy with a diameter of more than 100 km occurs and the geostrophic vorticity

is negative in the SCS2, causing the thermocline to deepen and thicken (Fig. 2b). After 20 December 1998, geostrophic vorticity becomes positive (Fig. 4b), causing the thermocline to become shallower at this station than the other two stations (Fig. 2b and Fig. 4b), regardless winter heat loss trying to deepen the thermocline. From the end of January to early February 1999, the upper boundary of the thermocline rises and falls rapidly during 10 day. Such a variation may be caused by alternation of the negative and positive vorticities in same period (Fig. 4b). After the end of January, the upper part of the thermocline rises due to positive vorticity (Fig. 2b and Fig. 4b). In March 1999, the upper boundary of the thermocline is very close to the sea surface. A new thermocline formed above 60 m. This is mainly due to the intensive sea surface heating (Yang, et al 1999). The positive vorticity (Fig. 4b) also facilitated the rising of thermocline. The double-thermocline structure is very evident and both maximum of vertical gradient of temperature are larger than $0.1^{o}Cm^{-1}$ and the thermocline gap is above 15 m (from -55 m to -70 m) (Fig. 5).

SCS3

The thermocline gradually rises from April 1998. In early June 1998, when the rising of thermocline stops, the upper boundary of the thermocline reaches at 20-30 m (Fig. 2c). This is caused by two mechanisms: positive geostrophic vorticity at early June (Fig. 4c) and increasing solar radiation (shallow mixed layer). On 10 November 1998, the upper and lower boundaries of the thermocline rise to 30 m and 100 m due to the positive vorticity (Fig. 4c). The thermocline rises again from mid January until the end of January 1999 (Fig. 2c) due to positive geostrophic vorticity. The upper and lower boundaries of the thermocline are shallower than 30 and 130 m, respectively. In February 1999, the geostrophic vorticity changes from positive to negative (Fig. 4c). Together with the heat loss at the sea surface, the thermocline deepens rapidly (Fig. 2c) with its upper boundary downward from 20 m (early January 1999) to 80 m (mid February 1999) and its lower boundary downward from 130 m (early January 1999) to 200 m (mid February 1999). From the end of March to early April 1999, the occurrence of the double-thermocline structure is solely caused by strong sea surface heating. In this case, the thermocline gap is above 30 m (from -50 m to -80 m) (Fig. 5).

Conclusions

Based on one-year (Feb. 1998 - Mar. 1999) ATLAS buoy (three stations) and satellite T/P-ERS data, we investigated the seasonal and intraseasonal thermocline variabilities and forcing factors. Our results are summarized as follows.

(1) The seasonal variation of the thermocline in the central SCS is mainly caused by seasonal variabilities of the surface wind stress and net heat flux. While the intraseasonal variation (time scale of 1-2 months) of the thermocline is mainly caused by mesoscale eddies and intraseasonal variation of the net heat flux. The seasonal thermocline variability is stronger in northern than in southern part of central SCS.

(2) Thermocline thickness of the central SCS is mainly determined by the sea surface net heat flux. In winter, the thermocline is deeper and thinner due to great amount of heat loss.

(3)The variation of the thermocline depth is closely related to SSH with correlation coefficient of -0.462 (SCS1), -0.88 (SCS2) and -0.699 (SCS3) (confidence level exceeding 95%) at the three ATLAS buoy stations, respectively. The themocline variabilities are 437, 170 and 240 times as large as that of the SSH variabilities at the three ATLAS stations.

(4) The depth of the 22°C isotherm has a close relationship with the surface geostrophic vorticity (representing mesoscale eddies) with correlation coefficients of 0.573, 0.512 and 0.481 at the three ATLAS stations, respectively. The first baroclinic mode, represented by the ratio between SSH and thermocline depth anomaly, is dynamically important in the central SCS. Furthermore, the intraseasonal variability of the thermocline can be inferred from the intraseasonal variability of the satellite-derived SSH data.

(5) The main type of double-thermocline structure are found with the gap between the upper and lower thermoclines above 80 m deep in Spring, wing to strong solar radiation.

In this paper, the mechanism of thermocline variation in intraseasonal and seasonal time scales is discussed. In particular, the mechanism of double-thermocline is elucidated in spring. Further study should be concentrated on the variation and formation mechanism of mesoscale eddies.

Acknowledgments. Ministry of Science and Technology of China supported this study through SCSMEX and National Key Program for Developing Basic Science "G1999043807". We thank Prof. C-Y. Tang at the National Taiwan University for providing processed buoy data and thank Prof. Ruixin Huang for useful suggestions. Peter Chu was supported by the Office of Naval Research and the Naval Oceanographic Office.

References

Chu, P.C., C.W. Fan, C.J. Lozano, and J. Kerling, An airborne expandable bathythermograph (AXBT) survey of the South China Sea May 1995, *J. Geophys. Res., 103,* 21637-21652, 1998.

Chu, P.C., N.L. Edmons, and C.W. Fan, Dynamical mechanisms for the South China Sea seasonal circulation and thermohaline variabilities, *J. Phys. Oceanogr., 29,* 2971-2989, 1999.

Gill, A.E. *Atmosphere-Ocean dynamics,* 662 pp., Academic, New York, 117-127, 1982.

Liu, Q.Y., H.J. Yang, and Q. Wang, Dynamic characteristics of seasonal thermocline in the deep sea region of the South China Sea, *Chinese. J. Oceanol., 18,* 104-109, 2000.

Liu, Z.Y., H.J. Yang and Q.Y. Liu, Regional dynamics of seasonal variability of SSH in the South China Sea, *J. Phys. Oceanogr., 31,* 272-284, 2001.

Qiu, Z., X.Z. Xu, and X.M. Long, The characteristics of thermocline in Nansha Island in September,1994, *Tropic Oceanography, 15(2),* 61-66, 1996.

Xu, X.Z., Z. Qiu, and X.M. Long, The radical characteristics and the one-dimentional calculated pattern of the South China Sea thermocline, *Oceanologia et Limnologia Sinica, 24(5),* 494-502, 1993.

Yang, H.J., Q.Y. Liu, and X.J. Jia, On the upper oceanic heat budget in the South China Sea: Annual cycle, *Adv. Atmos. Sci., 16,* 619-629, 1999.

Qinyu Liu, Yinglai Jia, Penghui Liu, Qi Wang, Physical Oceanography Laboratory, Ocean University of Qingdao, Qingdao, 266003, China (e-mail: liuqy@lib.ouqd.edu.cn)

Peter C. Chu, Department of Oceanography, Naval Postgraduate School, Monterey, CA, U.S.A.

(Received March 15, 2001; revised August 23, 2001;
accepted September 7, 2001.)